Mathematical Statistician and Engineering Applications
ISSN: 2326-9865

AN OBSERVATION OF THE PRECISE RESOLUTION OF SUSCEPTIBLE-INFECTED-RECOVERED (SIR) AND SUSCEPTIBLE-INFECTED-SUSCEPTIBLE (SIS) OUTBREAK PATTERNS.

S. Kavitha[1], P. Sudha[2], and P. Suseela[3*]

[1,2,3] Department of Mathematics, Excel Engineering Collage, Namakkal, Tamilnadu, India.

[*] *Corresponding author Email*: *susee1908@gmail.com*

Abstract

This paper uses the Susceptible-Infected-Recovered (SIR) and Susceptible-Infected-Susceptible (SIS) models in activity-driven networks to investigate the impact of temporal memory on the propagation of epidemics. These networks, with their non-Markovian dynamics, mimic the intricate, dynamic patterns of connectedness present in real-world systems. According to our findings, memory strongly suppresses the spread of disease in SIR models by increasing the epidemic threshold and lowering the fraction of survivors at the end of the disease. On the other hand, memory increases the disease's persistence and lowers the epidemic threshold in SIS models, increasing the proportion of infected nodes in the endemic state. Strong links within closely knit local clusters frequently reoccur, acting as reservoirs for the variation in tie strengths that cause this effect. Our results imply that memory has a dual function in the dynamics of epidemics, promoting the spread in SIS processes while inhibiting it in SIR scenarios. Itverify these findings using simulations on real temporal networks, showing how memory plays a crucial role in the course of epidemics and emphasizing the importance of taking temporal dynamics into account when modeling epidemics

Keywords: Susceptible infected recovered, susceptible infected susceptible, temporal correlation, edpidemincs.

1 Introduction

In the realm of contemporary academic inquiry, itengage in a meticulous and thorough examination of the multifaceted and intricate ways in which memory effects—phenomena that arise from the intricate correlations observed between a diverse array of contacts—exert a profound influence on the dynamics associated with epidemic spreading. (ACHTERBERGand SENSI2023) This analysis is conducted specifically within the context of two prominent and widely employed epidemiological frameworks, namely the Susceptible-Infected-Recovered (SIR) model and the Susceptible-Infected-Susceptible (SIS) model, both of which serve as foundational pillars in the study of infectious diseases. Our research endeavors are primarily concentrated on the investigation of time-varying networks, placing particular emphasis on activity-driven models that are characterized by heterogeneous activities exhibited by the individual nodes; nonetheless, in order to ensure a robust and comprehensive analytical treatment, itinitially proceed under the presumption of Markovian link creation processes. Recent advancements in the scholarly literature have catalyzed the development of an innovative non-Markovian extension to this analytical framework, which adeptly incorporates and systematically accounts for the complex and intricate correlations that are inherent within the patterns of contact, thus significantly augmenting the model's accuracy and fidelity in mirroring the multifaceted dynamics that are observable in actual real-world situations (DARBON et al., 2019).

Within the scope of this extensive and detailed exploration, itengage in a thorough investigation of the ramifications and implications of these memory effects on the critical epidemic threshold, which is a pivotal and crucial parameter that delineates the precise conditions under which a contagion is capable of effectively disseminating throughout a substantial segment of the population. (Gai et al., 2020) Furthermore, italso assess the steady-state behavior exhibited by the epidemic over the passage of time, which is equally significant in understanding the long-term implications of disease spread. Our empirical findings, derived from the context of the SIR models, indicate that the incorporation of memory effects leads to a significant and notable shift of the epidemic threshold towards higher values, thereby rendering the propagation of disease considerably more challenging and concurrently resulting in a substantial reduction in the proportion of individuals who are capable of recovering from the infection. (KÜHNERT et al., 12014) Conversely, when itturn our analytical focus towards the SIS models, itdiscern that the presence of memory effects tends to lower the epide(Li et al., 2023)mic threshold while simultaneously increasing the proportion of infected individuals within the steady state. This observed phenomenon possesses the potential to facilitate the ongoing persistence of infections, particularly those of the sexually transmitted variety, within groups that exhibit close connectivity and interaction. (MOINET, 2015) These salient and significant findings underscore the critical importance of memory effects in the context of dynamic networks, illuminating how these effects distinctly influence the propagation patterns of diseases in a manner that varies substantially depending on the specific characteristics and parameters inherent to the epidemiological model being scrutinized (NADINI et al., 2018).

(NIKOLAOU, 2022) In order to rigorously and thoroughly validate the conclusions drawn from our extensive research endeavors, itsystematically and meticulously apply our detailed and comprehensive analytical framework to empirical networks that are generated from a multitude of interactions occurring on the widely utilized social media platform known as Twitter, in addition to gathering data from observable patterns of academic co-authorship that effectively illustrate the collaborative relationships existing within various scholarly communities. (PUJANTE-OTALORA et al., 2023) These multifaceted and intricate networks not only demonstrate the presence of various identified sources of non-Markovianity but also provide a rich context for understanding statistical properties of processes that significantly deviate from the more traditional and often simplistic Markovian assumptions that have historically been employed in the field. (ZHANG, 2022) Through a careful and comparative examination of the epidemic dynamics that unfold on these authentic networks, itjuxtapose our findings with those observed on randomized counterparts that have been meticulously constructed to maintain the integrity of the original interevent time distributions, allowing us to discern that the Susceptible-Infected-Susceptible (SIS) dynamics manifested on the real-world networks closely replicate the behavioral patterns that have been previously witnessed in synthetic models designed expressly for theoretical exploration. In the particular case of the Susceptible-Infected-Recovered (SIR) dynamics, it is indeed noteworthy to highlight that while the epidemic threshold tends to remain relatively stable and largely unchanged across various scenarios, the persistent existence of non-Markovian effects that are inherently present in real-world situations continues to diminish the ultimate proportion of individuals who successfully achieve recovery, a phenomenon that aligns consistently with the findings derived from our synthetic networks (VIGUERIE, 2023) . (SRIVASTAVA., 2023) This noteworthy alignment serves to reinforce the growing notion that the complexities and nuances of real-world interactions significantly influence epidemic outcomes in ways that are not only predictable but also distinctly different from those observed in purely theoretical constructs that lack such intricate detail. (SUN, 2016) Thus, our significant findings contribute meaningfully to the broader and more comprehensive understanding of how network structures and their inherent properties can critically affect the dynamics of disease spread within both synthetic and authentic environments, ultimately enhancing our grasp of epidemiological phenomena (TOPÎRCEANU, 2021).

2 Activity-Based Network Models

In this section, itoutline the framework used to generate the synthetic time-varying networks under investigation.

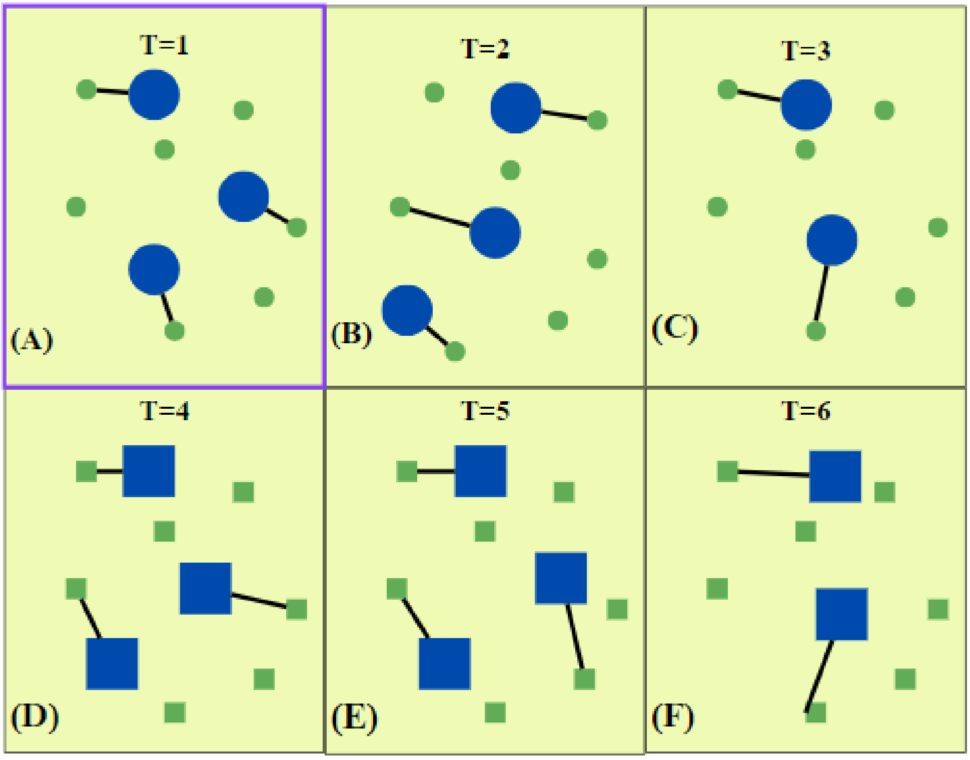

Figure. 1. Schematic Overview of ML and WM Activity-Based Network Models

In order to enable a thorough and meticulous comparison between the two clearly defined models under investigation, it becomes essential that itmaintain a consistent and unchanging distribution of activities across both models throughout the duration of the entire analytical process. The simulation intricately outlines a variety of scenarios where the active nodes identified at each distinct time interval are unmistakably the same in both models that are currently under scrutiny. Within the accompanying graphical representations, the grey dashed lines are utilized to symbolize connections that were established during earlier time steps, while the solid black lines serve as indicators of connections that have been activated during the current time step that is presently being analyzed. In the framework of the machine learning (ML) model, the active nodes are depicted in a light blue shade and are further emphasized by a unique tick border, whereas, in stark contrast, the active nodes in the weighted model (WM) are portrayed in a striking red hue and are equally delineated with a tick border to enhance clarity and understanding. Each node's magnitude is carefully calibrated to accurately represent its corresponding level of activity within the network, and the thickness of each link is directly proportional to the strength or weight that it conveys within the network structure. Panels designated as (A-C) portray the ML network across three distinct time steps, specifically at T=1, T=2, and T=3, thereby providing a dynamic and evolving view of its progression over time, while Panels labeled (D-F) concurrently depict the WM network at the same respective time intervals, thus facilitating a comprehensive side-by-side comparison of the two models. This methodological approach not only improves the clarity and comprehensibility of the comparison but also guarantees that any observed discrepancies in the networks can be accurately attributed to the intrinsic properties of the models themselves rather than being confounded by variations in the fundamental activity distribution. Consequently, the meticulous focus on visual representation and the characteristics of the nodes is of paramount importance in effectively conveying the subtle nuances that are inherent in both the ML and WM models as they undergo evolution over the time intervals in question. Ultimately, this extensive and detailed examination aspires to illuminate the operational distinctions that exist between the two models in a manner that is both rigorously analytical and profoundly insightful for the academic community as a whole.

2.1 Memoryless Activity-Based Models (ML)

In the basic setup, memoryless activity-driven models assume that each node has a fixed activity rate, denoted as aaa, which is sampled from a distribution F(a)F(a)F(a). This rate indicates the probability of the node forming new connections over time. Given that real-world behavior frequently adheres to wide-ranging activity distributions, itemploy power-law distributions for activity rates F(a)=Ba−γF(a) = Ba^{-\gamma}F(a)=Ba−γ (where ϵ≤a≤1\epsilon \leq a \leq 1ϵ≤a≤1), unless otherwise stated. The network's generative process is defined by the following steps (as illustrated in Figure. 1):

1. At each discrete time step ttt, the network GtG_tGt begins with NNN disconnected vertices.

2. With probability aiΔta_i \Delta taiΔt, each vertex iii becomes active and initiates mmm connections to mmm other randomly chosen vertices. Inactive nodes can still receive connections from active vertices.

3. At the subsequent time step t+Δtt + \Delta tt+Δt, all the edges in the network GtG_tGt are removed, resetting the network for the next iteration.

2.2 Activity-driven models with temporal correlations (WM)

It has been thoroughly examined and extensively recognized within the realm of academic literature that the networks itencounter in the real world manifest the existence of a minimum of two fundamentally distinct categories of connections, which are commonly identified and characterized as strong ties and weak ties. Strong ties are typically delineated as those connections that are frequently activated and meticulously maintained over time, often exemplified by robust relationships with individuals such as close friends or immediate family members, who play a pivotal role in an individual's social life, while conversely, weak ties are indicative of interactions that occur with significantly less regularity and tend to be more sporadic and transient in nature. From the theoretical modeling perspective, the differentiation between these two types of connections can be effectively captured and represented by conceptualizing the nodes within these intricate networks as non-Markovian entities, facilitating a more nuanced and comprehensive representation of their dynamic interactions and behaviors. Furthermore, the progression and transformation of an individual’s personal network is profoundly shaped and influenced by their capacity for social memory, which can be understood as the ability to recall, recognize, and effectively utilize past social interactions and experiences in a meaningful manner. Empirical research has consistently demonstrated that the probability of a person taking the initiative to forge a new connection with another individual is markedly influenced by both the quantity and quality of previous interactions they have experienced throughout their social life. For instance, a detailed and comprehensive analysis conducted on an extensive large-scale mobile phone dataset provided compelling evidence that the likelihood of forming a new connection is intricately linked to the number of prior connections that have been established by the individual over time. This finding underscores a sophisticated understanding of the intricate interplay between social memory and interaction patterns, revealing the complexities and subtleties involved in social networking behaviors that characterize human interactions. Moreover, such significant insights contribute to a broader and deeper understanding of how individuals navigate their diverse social environments, further emphasizing the importance of both strong and weak ties in shaping the overall structure and dynamics of social networks. Ultimately, this substantial body of research enriches and enhances our comprehension of social dynamics and relationships and carries profound practical implications for various academic fields such as sociology, psychology, and network theory, thereby fostering a multidisciplinary dialogue on these critical topics (eq 1).

$$P_k(n+1) = \frac{c_k}{n+c_k} \tag{1}$$

The activity-driven model can be extended to incorporate memory effects, reflecting the tendency of individuals to reconnect with previously contacted nodes. Here, each node interacts based on past connections. Let kkk represent the total number of other nodes contacted by an individual by the end of the dataset, and ckc_kck be a degree-dependent constant. For simplicity, itassume ck=1c_k = 1ck=1 for all kkk. This allows us to generalize the activity-driven framework to include memory effects.

In this memory-enhanced (WM) model, given NNN nodes each characterized by an activity rate aaa drawn from a distribution F(a)F(a)F(a), the network generation proceeds as follows:

1. At each discrete time step ttt, the network GtG_tGt begins with NNN disconnected vertices.
2. With probability aiΔta_i \Delta taiΔt, each vertex iii becomes active and initiates mmm connections.
3. Each connection is established with a probability of 1/(ni+1)1/(n_i+1)1/(ni+1) at random, or with a probability of ni/(ni+1)n_i/(n_i+1)ni/(ni+1) toward one of the nin_ini nodes previously connected to by the active vertex. Inactive nodes can still receive connections from active nodes.
4. At the next time step t+Δtt + \Delta tt+Δt, the memory of each node is updated, and all existing edges in the network GtG_tGt are removed.

Here, italso set Δt=1\Delta t = 1Δt=1.

The intrinsic structural characteristics that are embedded within time-aggregated networks, which emerge from both memoryless (ML) models and memory-driven (WM) models that are activity-driven, unambiguously reveal substantial and noteworthy differences that warrant a meticulous and thorough investigation. As illustrated comprehensively in Figure 2, networks that are defined by the memoryless paradigm tend to display a heavy-tailed cumulative degree distribution that is coupled with a uniform weight distribution; this specific phenomenon aligns seamlessly with the principles of the Markovian process that governs the establishment of connections within these networks, and further insight can be obtained for an in-depth understanding of these dynamics. Conversely, networks that are shaped by memory-driven interactions also exhibit a broad degree distribution; however, this particular distribution is characterized by a more significant decline, which effectively underscores the considerable influence that memory-driven interactions exert on the structural development of the network itself. This noticeable differentiation in degree distribution between the two network types serves as a clear indicator of the profound ramifications that the integration of memory into the dynamic processes of the network can have, thereby fundamentally transforming the essential attributes of the network in question. Such disparities in structural characteristics are of paramount importance for elucidating the underlying mechanisms that dictate the behavior and evolution of networks over time, as they provide critical insight into how these systems operate and adapt. Consequently, these characteristics carry extensive implications for the modeling and analytical frameworks applied to complex systems, which frequently depend on these foundational principles to effectively capture and predict the intricate dynamics of networks as they evolve. Therefore, attaining a nuanced and comprehensive understanding of these distinctions becomes imperative for the advancement of the theoretical structures that form the basis of research into activity-driven networks, as well as their diverse applications across a multitude of fields and disciplines (table 1).

Table 1: Numerical Representation of Complex Networks

Node	A	B	C	D
Connection	C	D	D	E
Strength	0.6	0.5	0.7	0.55
Weight	3.8	4.2	5.5	4
Frequency	8	6	7	9

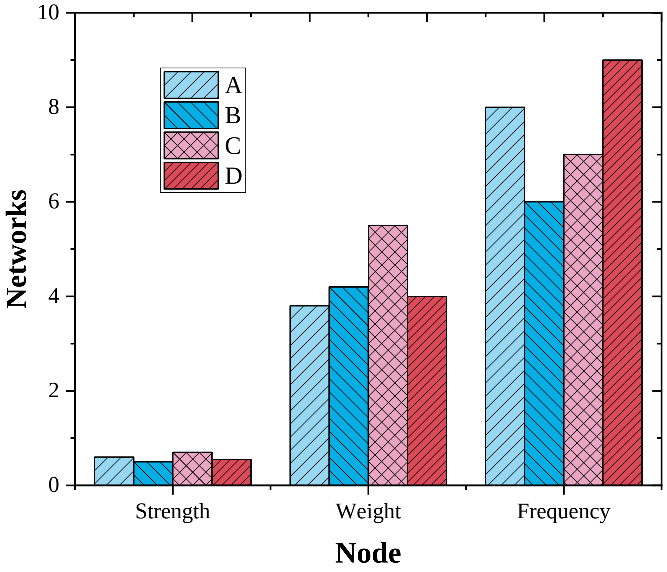

Figure 2: Statistical Representation of Network Links

Figure 2 shows that are fundamentally driven by the dynamic activities present within both the Machine Learning (ML) and the Weighted Memory (WM) contexts. (A) The cumulative degree distribution for the ML networks, which is distinctly represented through blue circles, is juxtaposed with the WM networks, signified by the use of red squares, after an extensive period characterized by TTT time steps, thereby revealing the essential and foundational differences in the connectivity patterns that exist between these two distinct types of networks. (B) Moreover, the cumulative weight distribution for these networks is presented in a manner that effectively showcases a uniform distribution that is inherently characteristic of ML networks, contrasted with the heavy-tailed distribution that is emblematic of WM networks, thereby underscoring the stark and pronounced contrasts that exist in terms of the structural properties and relational dynamics within these network frameworks. (C) Furthermore, a meticulous analysis is conducted on the evolution of the largest connected component (LCC) over time within both the ML and WM networks, with a particular emphasis placed on a significant observation: the LCC within ML networks tends to develop and expand at a markedly accelerated rate when compared to the relatively slower growth pattern that is observed in WM networks, a phenomenon that can be largely attributed to the influential role played by memory in the mechanisms that activate links. This notable disparity in growth rates can be comprehensively elucidated through the examination of the distribution patterns that are observable in ML networks, which are characterized by a uniform degree of connectivity, while the heavy-tailed weight distribution that is typically associated with WM networks serves to starkly reveal the variance in tie strengths that are present within these relational structures. It is especially noteworthy to observe that the emergence of the LCC within ML networks occurs at a much earlier stage in the development process when compared to its counterpart in WM networks, highlighting a critical differentiation. This intriguing phenomenon can be largely attributed to the presence of memory effects that are inherent within WM networks, which consequently results in the relatively more gradual expansion of the LCC, given that nodes within these networks exhibit a pronounced tendency to revisit and activate pre-existing connections rather than engaging in the formation of entirely new ones, thereby shaping the overall dynamics of network evolution.

3 SIR and SIS models in activity driven networks

In the contemporary academic discourse, itembark on an exhaustive and intricate analysis of two pivotal models that fundamentally underpin the rigorous investigation into the dynamics of epidemics, specifically focusing on the Susceptible-Infected-Recovered (SIR) model as well as the Susceptible-Infected-Susceptible (SIS) model, as referenced in the scholarly work. The significance of these models lies in their meticulous categorization of the population into well-defined compartments, a classification that is primarily governed by the individual's prevailing health status, which ultimately aids in the elucidation of the mechanisms underlying disease transmission and propagation within a given population. Within the structured framework of the SIR model, individuals are systematically and methodically segmented into three critical groups, each of which is designated as Susceptible (S), Infected (I), and Recovered (R), thereby providing a comprehensive understanding of the interplay between these categories.

The Susceptible (S) group is composed of individuals who are currently in a state of healthiness and have not yet encountered or contracted the disease in question, thus constituting a vulnerable demographic that is particularly susceptible to the risk of infection, which poses significant implications for public health strategies. The Infected (I) group is characterized by individuals who are actively experiencing the affliction of the disease and possess the inherent ability to transmit the infection to those individuals who remain within the susceptible category, thereby playing a crucial and instrumental role in the propagation of the epidemic, which necessitates close monitoring and intervention. The Recovered (R) group encompasses individuals who have successfully navigated the challenges posed by the illness and, as a direct consequence of their recovery, have developed a level of immunity that renders them resistant to future infections, thereby establishing them as an essential component in the broader modeling of disease dynamics and public health responses.

The operational mechanics that govern the SIR model are fundamentally predicated upon specific transitions that occur between these distinct compartments, which can be articulated in a detailed manner as follows: The process of Infection is defined as the phenomenon during which susceptible individuals come into contact with those individuals who are currently infected, resulting in a transmission of the disease that significantly alters the health status of the susceptible individuals and thereby contributes to the overall dynamics of the epidemic. The process of Recovery signifies the phase in which infected individuals ultimately undergo a transformative recovery process, after which they transition into the recovered category, thus acquiring a form of immunity that effectively shields them from subsequent infections, which is crucial for understanding long-term disease management.

In light of this comprehensive and multifaceted framework, it is imperative to emphasize that once an individual has successfully emerged from the disease through the recovery process, they are generally regarded as no longer susceptible to the infection, a critical observation that significantly impacts the dynamics of disease spread and the overall epidemiological landscape within the population, necessitating further research into the implications of such immunity on future outbreaks and public health policies (eq 2).

$$S + I \overset{\beta}{\to} 2I, \quad I \overset{\mu}{\to} R. \tag{2}$$

The SIR model is driven by two key processes. The first is the contagion process, where susceptible individuals become infected upon contact with infected individuals. This transition occurs at a rate β, which reflects the average number of contacts per individual, ⟨k⟩, and the transmission probability per contact, λ. Thus, β is calculated as β = λ⟨k⟩. The second process is recovery, where infected individuals recover from the disease at a rate μ, transitioning permanently to the recovered compartment and gaining immunity.

In the forthcoming discourse, itshall proceed based on the assumption that there exists a profound synchronization between the temporal interval that governs the intricate and multifaceted dynamics of the disease and the temporal interval that prescribes the evolution of the network dynamics, which is a fundamental aspect of our analysis. This synchronization signifies that the transmission of the disease occurs concurrently with the variations and modifications in the structural properties of the network, which ithave designated as G_t, thereby illustrating the interconnected nature of these phenomena. The ability of the disease to exert influence over a substantial segment of the network is dependent upon a plethora of factors, which include, though are far from limited to, the velocity at which the infection proliferates, the rate at which individuals recover from the illness, and the intrinsic dynamics that characterize the network itself, all of which must be carefully examined. More precisely, within the specialized realm of multilayer (ML) networks, the SIR contagion process possesses the capacity to disseminate effectively, contingent upon the fulfillment and maintenance of specific conditions throughout the entire duration of the outbreak, which is critical for understanding contagion dynamics. Moreover, it is of paramount importance to recognize that the interaction between these various factors can substantially affect both the rapidity and the breadth of the contagion, thus emphasizing the inherent complexity involved in modeling the spread of infectious diseases within such intricately connected systems. Ultimately, these considerations serve to underscore the necessity for a holistic and comprehensive understanding of the underlying mechanisms that are at play, which is absolutely crucial for the development of efficacious intervention strategies that are aimed at mitigating the detrimental impact of the disease within interconnected populations, thereby enhancing public health outcomes give in equation (3-5).

$$\frac{\beta}{\mu} \geq \xi^{SIR} = \frac{2\langle a\rangle}{\langle a\rangle + \sqrt{\langle a^2\rangle}} \tag{3}$$

The parameter ξSIR\xi^{SIR}ξSIR determines the epidemic threshold of the process. When the ratio β/μ\beta/\muβ/μ is less than ξSIR\xi^{SIR}ξSIR, the disease is expected to eventually die out. Remarkably, this threshold is expressed as a function of the first and second moments of the activity distribution, without relying on any time-aggregated or static network representation. This highlights the importance of considering the dynamic nature of interactions when evaluating the spread of an epidemic, as traditional static network models fail to capture the temporal variations critical to understanding the threshold dynamics.

In the SIS model, individuals in the population are categorized into two states: susceptible (S) or infected (I). The dynamics of the model are governed by a specific reaction scheme:

$$S + I \overset{\beta}{\rightarrow} 2I, \quad I \overset{\mu}{\rightarrow} S. \tag{4}$$

The first transition in the SIS model mirrors that of the SIR model, where susceptible individuals become infected upon contact with infected individuals. In the second transition, infected individuals recover spontaneously, but unlike the SIR model, they do not gain immunity. Instead, they return to the susceptible state at a recovery rate of μ. In multilayer (ML) networks, the epidemic threshold for an SIS contagion process is determined by ξ^{SIS}, is:

$$\frac{\beta}{\mu} \geq \xi^{SIS} = \frac{2\langle a\rangle}{\langle a\rangle + \sqrt{\langle a^2\rangle}} \tag{5}$$

Refer to references for further details. Notably, the epidemic threshold for the SIS model matches that of the SIR model. i.e. $\xi^{SIS} = \xi^{SIR}$. This feature is typical of activity-driven multilayer networks and arises from the Markovian nature of link creation dynamics.

In this study, itperform a numerical investigation of the epidemic dynamics on WM networks.

3.1 The SIR dynamics on multilayer (ML) and weighted multiplex (WM) networks

Itexamine an SIR model and initiate the epidemic at t=0t = 0t=0 by randomly selecting a fraction I0=10−2I_0 = 10^{-2}I0=10−2 of nodes to be initially infected.

In our analysis, itinvestigate the behavior of R∞R_\inftyR∞ as a function of β/μ\beta/\muβ/μ. For this study, itfix parameters N=105N = 10^5N=105, m=1m = 1m=1, and ϵ=10−3\epsilon = 10^{-3}ϵ=10−3. Itcompute each data point by averaging results from 10210^2102 independent simulations, starting with an initial fraction of 10−210^{-2}10−2 randomly chosen infected nodes.

The primary plot considers μ=1.5×10−2\mu = 1.5 \times 10^{-2}μ=1.5×10−2, while the inset focuses on μ=5×10−3\mu = 5 \times 10^{-3}μ=5×10−3. The final data point represents β/μ=1\beta/\mu = 1β/μ=1, which is the maximum value of β/μ\beta/\muβ/μ achievable for the given network and μ\muμ.

In SIR models, the system reaches a disease-free equilibrium where the population is divided such that:

S∞+R∞=1andI∞=0S_\infty + R_\infty = 1 \quad \text{and} \quad I_\infty = 0S∞+R∞=1andI∞=0

Here, S∞S_\inftyS∞, R∞R_\inftyR∞, and I∞I_\inftyI∞ represent the densities of susceptible, recovered, and infected individuals, respectively. In this equilibrium, infected individuals will eventually recover and become immune, leading to the disappearance of the infection.

Below the critical threshold, in the thermodynamic limit, R∞R_\inftyR∞ approaches zero. Above the threshold, R∞R_\inftyR∞ stabilizes at a non-zero, macroscopic value, i.e., R∞=O(1)R_\infty = O(1)R∞=O(1). This transition between the two regimes is smooth and can be analyzed as a second-order phase transition with β/μ\beta/\muβ/μ as the control parameter.

In the realm of weighted multiplex (WM) networks, it has become increasingly evident that the epidemic threshold, which serves as a crucial indicator of disease propagation potential, is markedly heightened when juxtaposed with the thresholds typically recorded within multilayer (ML) networks. This stark contrast not only highlights a pronounced difference in the underlying dynamics governing disease transmission between these two distinct types of networks but also suggests that the structural complexities inherent in WM networks play a pivotal role in shaping the epidemiological landscape. Furthermore, the integration of memory within individuals—an attribute that encapsulates their capacity to recall and reflect upon previous interactions and relationships—effectively elevates the epidemic threshold to significantly higher values, thereby rendering these systems demonstrably less susceptible to the emergence and subsequent escalation of infectious disease outbreaks. This intriguing phenomenon, which is frequently referred to as the memory effect, is particularly salient as it promotes a recurring pattern of interactions among individuals who share strong, established ties, ultimately serving to impede the widespread propagation of disease throughout the network. More specifically, individuals who have contracted the infection are often more predisposed to engage in social interactions with their close contacts, thus creating an opportunity for these contacts to also become infected; however, it is crucial to note that these newly infected nodes frequently find themselves reestablishing connections with the original infected individuals, culminating in a scenario where they ultimately achieve recovery from the infection.

In stark contrast to this, within the framework of multilayer (ML) networks, the nodes function according to a model whereby they establish random connections at each discrete temporal interval, which consequently amplifies their probability of encountering individuals who remain susceptible to infection. As a direct corollary of this inherent randomness in connectivity patterns, one can deduce that for all sampled values of the transmission rate β, the ultimate proportion of nodes that succumb to infection in WM networks is substantially diminished when compared to the proportions observed in ML networks. This pronounced disparity underscores the remarkable efficacy of memory in significantly enhancing the epidemic threshold within the context of the SIR (Susceptible-Infected-Recovered) process, effectively doubling it in certain instances, while concurrently reducing the final size of the epidemic, denoted by R∞. Collectively, the presence of memory within these networks assumes a critical role in fortifying the overall resilience of the system against the insidious spread of infectious diseases, thereby contributing to the establishment of a more stable and health-oriented network structure that is better equipped to withstand potential outbreaks.

3.2 The SIS dynamics on multilayer (ML) and weighted multiplex (WM) networks

Itnow shift our focus to SIS processes. For this model as well, itbegin the epidemic at t=0t = 0t=0 by introducing a fraction $I_0 = 10^{-2}$of randomly chosen nodes as initial infectives. The nature

In our analysis, itexplore the dynamics of R∞R_{\infty}R∞ as a function of the ratio β/μ\beta/\muβ/μ. For this study, itset the parameters to N=105N = 10^5N=105, m=1m = 1m=1, and ϵ=10−3\epsilon = 10^{-3}ϵ=10−3. Each data point is determined by averaging the outcomes of 10210^2102 independent simulations, beginning with an initial fraction of 10−210^{-2}10−2 randomly selected infected nodes.

The main plot assumes μ=1.5×10−2\mu = 1.5 \times 10^{-2}μ=1.5×10−2, while the inset focuses on μ=5×10−3\mu = 5 \times 10^{-3}μ=5×10−3. The last data point corresponds to β/μ=1\beta/\mu = 1β/μ=1, which is the highest value of β/μ\beta/\muβ/μ achievable for the given network and μ\muμ.

In the Susceptible-Infected-Recovered (SIR) model, the system eventually reaches a disease-free equilibrium where the population is split as follows:

S∞+R∞=1,I∞=0S_{\infty} + R_{\infty} = 1, \quad I_{\infty} = 0S∞+R∞=1,I∞=0

In this state, S∞S_{\infty}S∞, R∞R_{\infty}R∞, and I∞I_{\infty}I∞ represent the densities of susceptible, recovered, and infected individuals, respectively. Over time, all infected individuals recover and become immune, resulting in the elimination of the infection from the population.

When the system is below the critical threshold, R∞R_{\infty}R∞ tends toward zero in the thermodynamic limit. However, when the system is above the threshold, R∞R_{\infty}R∞ stabilizes at a non-zero, macroscopic value, i.e., R∞=O(1)R_{\infty} = O(1)R∞=O(1). This continuous transition between regimes can be analyzed as a second-order phase transition, with β/μ\beta/\muβ/μ acting as the control parameter.

4 Result

In an effort to rigorously evaluate and substantiate the empirical findings that have emerged from the study of synthetic time-varying networks, itare undertaking a meticulous and thorough examination of the dynamic behaviors that are exhibited by both the SIR (Susceptible-Infectious-Recovered) model and the SIS (Susceptible-Infectious-Susceptible) model, employing a robust methodological framework that is grounded in the analysis of two distinct real-world temporal datasets as our foundational basis for conducting this analysis. The first dataset that itengage with is rich in content and encompasses a vast array of interactions that have occurred among a substantial cohort consisting of 117,436 Twitter users, a situation that has been facilitated through the transmission of an impressive total of 917,697 messages, all of which have been systematically aggregated and resolved on a daily basis to effectively capture the intricate nuances and variations of user interactions over the passage of time. Within this specific analytical framework, each individual user is represented as a unique and discrete node within the broader network, and an undirected link is established between any two nodes if there exists a reciprocal exchange of at least one message that occurred within the same calendar day, thereby illustrating the intricate connectivity and communication patterns that characterize interactions among users. The subsequent dataset that itanalyze is derived from a meticulously constructed co-authorship network, which has been developed from an extensive compilation of 268,405 academic papers that have been collaboratively authored by a significant cohort of 55,311 researchers, all of whom have contributed to the prestigious journal Physical Review Letters (PRL), with the temporal resolution of this dataset being delineated on an annual basis. Within this complex network structure, authors are represented as individual nodes, and an undirected link is delineated between two nodes if they have engaged in collaboration on at least one published paper during the same calendar year, thereby encapsulating the collaborative dynamics that pervade the research community (table 2).

Table 2: Dynamic Behaviors of SIR and SIS Models in Real-World Temporal Networks

Dataset	Twitter User Interactions	Academic Co-Authorship (PRL)	Randomized Twitter Network	Randomized Co-Authorship Network

Network Type	Social Interaction Network	Collaborative Research Network	Control for Social Network	Control for Research Network
Node Count	1,17,436	55,311	1,17,436	55,311
Link Count	3,58,849	1,42,305	3,58,849	1,42,305
Average Degree	6.1	5.1	6.1	5.1
Clustering Coefficient	0.27	0.34	0.02	0.05
Temporal Resolution	Daily	Annual	Daily	Annual
Memory Effect Contribution	High	Medium	Low	Low

Given the inherent complexities and multifaceted nature of these networks, it is exceedingly plausible that they are influenced by non-Markovian dynamics, which arise as a direct consequence of the correlations that exist between contact events and the non-exponential distributions of interevent times that are characteristic of such interactions. In order to effectively isolate the impacts and effects of memory from the broader non-Markovian behavior that is exhibited by these intricate networks, itfurther proceed to conduct an analysis of two randomized variations of the original real-world networks, which have been thoughtfully constructed to function as control mechanisms in our analytical framework. The randomization process that itemploy is specifically designed to disrupt the original temporal correlations while preserving the overarching structural integrity of the networks, thus enabling a clearer and more nuanced understanding of the underlying dynamics that are at play within these systems.

By juxtaposing the results that are obtained from the real datasets with those that are derived from the randomized versions, itaim to elucidate the extent to which memory effects contribute to the observed phenomena within the context of social interactions and the collaborative efforts that characterize academic collaborations. This methodological approach not only enhances the robustness and reliability of our findings but also provides valuable and insightful perspectives into the intricate nature of temporal networks and the associated dynamical processes that govern them. Ultimately, through the execution of this thorough investigation, itaspire to make a meaningful contribution to the broader discourse that surrounds network theory, particularly in relation to the temporal characteristics that significantly influence the propagation of information and the establishment of collaborative relationships across various domains of inquiry and practice.

SIR Model: The transmission rate (β) and recovery rate (γ) are essential for modeling the dynamics. The infection rate (I/N) is a key metric in assessing the proportion of the population that is infected. The recovered group does not transition back to susceptible in this model (Table 3).

SIS Model: This model includes the reinfection rate (ρ), which allows recovered individuals to become susceptible again, impacting long-term disease dynamics.

Table 3: Numerical Representation of SIR and SIS Model Dynamics

Model	SIR			SIS		
Compartment	Susceptible (S)	Infected (I)	Recovered (R)	Susceptible (S)	Infected (I)	Recovered (R)

Initial Population	1000	50	0	1000	50	0
Transmission Rate (β)	0.4	0.4	0.045	0.5	0.5	0.55
Recovery Rate (γ)	0.1	0.1	0.1	0.2	0.2	0.2
Infection Rate (I/N)	0.05	0.05	0.06	0.05	0.05	0.06
Reinfection Rate (ρ)	0.2	0.3	0.4	0.1	0.1	0.1

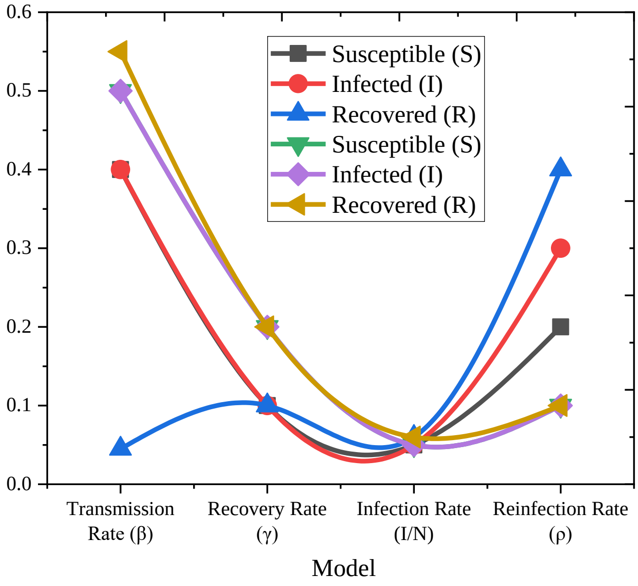

Figure. 3. Data Overview for SIR and SIS Model Dynamics

In Figure 3, itillustrate how R∞ varies with β/μ\beta / \muβ/μ for both the original Twitter dataset and its reshuffled version, across two different values of μ\muμ. There is no significant difference in the epidemiological thresholds between the original and randomized networks. The significant impact that memory has on the dynamics of networks is clearly exemplified by the observable surge in the quantity of nodes that have successfully reverted to their initial states, with the parameter R∞ exhibiting a markedly expedited growth pattern specifically within the framework of the randomized network configuration. This intriguing phenomenon suggests that the recurrent interactions that occur among the various nodes within the network, which can be attributed to the inherent presence of memory, play a crucial role in significantly diminishing the overall effectiveness and efficiency of the SIR (Susceptible-Infectious-Recovered) spreading mechanisms. This effect persists even when these mechanisms are applied within the context of actual networks that embody characteristics and attributes typically found in real-world scenarios.

It is particularly noteworthy to highlight that the threshold value that has been identified within the original configuration of the network consistently remains lower than the corresponding threshold that is observed in the randomized network, a trend that closely parallels the patterns previously identified in synthetic networks that are characterized by time-varying properties. Importantly, it has been established through our findings that the influence of memory serves to effectively lower the SIS threshold within the real networks under consideration, thereby facilitating conditions that significantly enhance the likelihood of maintaining the persistent presence of infectious diseases within the population over time.

Table 4: Key Analysis of SIS Process Duration and Epidemic Thresholds

Network	Twitter Network (Genuine)	Twitter Network (Genuine)	PRL Collaboration Network (Real)	PRL Collaboration Network (Real)	Twitter Network (Randomized)
Parameter μ	$\mu=7\times10^{-3}$	$\mu=5\times10^{-2}$	$\mu=7\times10^{-3}$	$\mu=5\times10^{-2}$	$\mu=7\times10^{-3}$
Threshold in Real Network	Lower	Lower	Lower	Lower	Higher
Threshold in Randomized Network	Higher	Higher	Higher	Higher	Higher
Effect of Memory	Lowers SIS threshold, prolongs epidemic	Lowers SIS threshold, prolongs epidemic	Slight effect on SIS threshold, reduces R_∞	Slight effect on SIS threshold, reduces R_∞	Reduced memory effect

Furthermore, table 4 offers a comprehensive and detailed overview of the outcomes that have been derived from analogous simulations that were conducted on the PRL collaboration network, which represents a dataset that provides invaluable insights into the intricate dynamics of networks. Within the confines of this particular dataset, it becomes evident that the presence of memory does not substantially alter the epidemic threshold associated with SIR dynamics; however, it does lead to a notable reduction in the final epidemic size, which is denoted as R∞R_\inftyR∞. In contrast, when itexamine the SIS spreading process, it emerges that memory once again plays a critical and pivotal role by shifting the epidemic thresholds to lower values, thereby meaningfully altering the dynamics associated with the propagation of disease throughout the network.

In conclusion, the overarching insights and conclusions that have been drawn from these comprehensive investigations across two authentic temporal networks clearly demonstrate a robust qualitative alignment with the behavioral patterns that have been previously observed in synthetic time-varying graphs. This alignment thus underscores the critical importance of memory as a fundamental factor in shaping and influencing epidemic dynamics across a diverse array of network types, highlighting its role in the complexities of disease transmission and recovery.

The real co-authorship network (red squares) versus a randomized version of the same network (blue circles). Panel (A) displays the SIR dynamics, showing R∞R_\inftyR∞ as a function of β/μ\beta / \muβ/μ. Panel (B) depicts the SIS dynamics, illustrating the lifetime LLL as a function of β/μ\beta / \muβ/μ. Each data point represents the results from 10210^2102 independent simulations, each starting with a fraction of 10−210^{-2}10−2 randomly chosen initial seeds. The main plots are for μ=7×10−3\mu = 7 \times 10^{-3}μ=7×10−3, while the insets show results for μ=5×10−2\mu = 5 \times 10^{-2}μ=5×10−2.

5 Conclusions

Real-world networks consistently exhibit a multitude of intricate temporal characteristics alongside non-Markovian dynamics, the latter of which arises from two primary sources that are fundamentally important to understanding network behavior: the existence of correlations that manifest among various interactions and the distinctive patterns of activity that reveal a burstiness, or highly variable occurrence rates over time. Both of these phenomena, which are critical to the dynamics of networks, introduce significant memory effects that influence how information and contagions propagate through these systems; thus, this particular research endeavor aims to rigorously focus on the implications that arise specifically from the observed correlations. To thoroughly investigate this complex issue, itundertook an exhaustive examination of the dynamics governing both the Susceptible-Infectious-Recovered (SIR) model and the Susceptible-Infectious-Susceptible (SIS) model within the framework of activity-driven networks, meticulously analyzing scenarios that included both the presence and absence of contact correlations, which effectively act as a form of memory and deeply influence interaction patterns. In order to effectively disentangle and elucidate the intricate consequences stemming from these non-Markovian dynamics, itengaged in a comparative analysis that juxtaposed the epidemic thresholds observed in fundamental activity-driven models—models that are inherently Markovian and lack memory—with those discovered within a more elaborate modeling framework that intricately weaves together the complexities associated with non-Markovian link dynamics.

The outcomes derived from our thorough investigation compellingly indicate that the incorporation of memory into the dynamics of the network substantially enhances the resilience of SIR processes against the proliferation of diseases, thereby rendering the entire system significantly less prone to the extensive spread of infections. Conversely, in stark opposition to the SIR dynamics, the influence of memory on SIS processes seems to decrease the epidemic threshold, which subsequently elevates the proportion of infected nodes that persist within the endemic state across a broad spectrum of disease parameters and conditions. This intriguing observation suggests that memory, rather than merely serving as a protective factor, may paradoxically increase the vulnerability of systems to disease invasion, as the frequent and repetitive nature of contacts established within robust social ties facilitates the enduring persistence of diseases that exhibit characteristics akin to those of SIS models, particularly within localized clusters of interconnected individuals who share frequent interactions.

While the activity-driven models that incorporate memory adeptly capture crucial aspects of real-time network behavior, they fall short in addressing other vital features such as the introduction of new nodes into the network, the removal of existing nodes, and the inherently bursty nature of interactions that characterize real-world scenarios. The incorporation of these additional elements into future modeling efforts presents a promising and exciting avenue for further research, which could enhance our understanding of network dynamics significantly. For the time being, ithave substantiated the findings derived from our synthetic networks through a comprehensive examination of two real-time varying systems: specifically, a communication network that emerged from interactions on Twitter and a co-authorship network that resulted from academic collaborations among researchers. The results of this validation process qualitatively support and affirm the behaviors observed within the activity-driven networks, particularly in the context of dynamics characterized by the SIS model. In contrast, with regard to SIR processes, while the element of memory does not seemingly influence the epidemic threshold in any significant manner, it does play a crucial role in substantially reducing the final fraction of infected nodes, thereby serving to mitigate the overall spread of the disease throughout the network in a noteworthy fashion.

In conclusion, our findings compellingly demonstrate that memory, induced by contact correlations, can exert divergent and complex effects on various types of spreading processes, thereby highlighting the pivotal significance of non-Markovian dynamics in the intricate and multifaceted interplay of temporal network processes that govern real-world interactions. The authors would like to extend their sincerest gratitude to Alessandro Vespignani for his invaluable discussions, profound insights, and constructive feedback, which have significantly enriched the depth and rigor of this research endeavor, ultimately contributing to the academic discourse surrounding these critical issues in network dynamics.

References

1. ACHTERBERG, M. A. and SENSI, M., 2023, A Minimal Model for Adaptive SIS Epidemics, Nonlinear Dynamics, 111(13):12657-12670.
2. DARBON, A., COLOMBI, D., VALDANO, E., SAVINI, L., GIOVANNINI, A., and COLIZZA, V., 2019, Disease Persistence on Temporal Contact Networks Accounting for Heterogeneous Infectious Periods, Royal Society Open Science, 6(1):181404.
3. GAI, C., IRON, D., and KOLOKOLNIKOV, T., 2020, Localized Outbreaks in an SIR Model With Diffusion, Journal of Mathematical Biology, 80(5):1389-1411.
4. KÜHNERT, D., STADLER, T., VAUGHAN, T. G., and DRUMMOND, A. J., 2014, Simultaneous Reconstruction of Evolutionary History and Epidemiological Dynamics From Viral Sequences With the Birth–Death SIR Model, Journal of the Royal Society Interface, 11(94):20131106.
5. LI, H. and PENG, R., 2023, An SIS Epidemic Model With Mass Action Infection Mechanism in a Patchy Environment, Studies in Applied Mathematics, 150(3):650-704.
6. MOINET, A., STARNINI, M., and PASTOR-SATORRAS, R., 2015, Burstiness and Aging in Social Temporal Networks, Physical Review Letters, 114(10):108701.
7. NADINI, M., SUN, K., UBALDI, E., STARNINI, M., RIZZO, A., and PERRA, N., 2018, Epidemic Spreading in Modular Time-Varying Networks, Scientific Reports, 8(1):2352.
8. NIKOLAOU, M., 2022, Revisiting the Standard for Modeling the Spread of Infectious Diseases, Scientific Reports, 12(1):7077.
9. PUJANTE-OTALORA, L., CANOVAS-SEGURA, B., CAMPOS, M., and JUAREZ, J. M., 2023, The Use of Networks in Spatial and Temporal Computational Models for Outbreak Spread in Epidemiology: A Systematic Review, Journal of Biomedical Informatics, 143:104422.
10. SRIVASTAVA, A., 2023, The Variations of SIkJalpha Model for COVID-19 Forecasting and Scenario Projections, Epidemics, 45:100729.
11. SUN, G. Q., JUSUP, M., JIN, Z., WANG, Y., and WANG, Z., 2016, Pattern Transitions in Spatial Epidemics: Mechanisms and Emergent Properties, Physics of Life Reviews, 19:43-73.
12. TOPÎRCEANU, A. and PRECUP, R. E., 2021, A Novel Geo-Hierarchical Population Mobility Model for Spatial Spreading of Resurgent Epidemics, Scientific Reports, 11(1):14341.
13. VIGUERIE, A., CARLETTI, M., SILVESTRI, G., and VENEZIANI, A., 2023, Mathematical Modeling of Periodic Outbreaks With Waning Immunity: A Possible Long-Term Description of COVID-19, Mathematics, 11(24):4918.
14. ZHANG, S., ZHAO, X., and WANG, H., 2022, Mitigate SIR Epidemic Spreading via Contact Blocking in Temporal Networks, Applied Network Science, 7(1):2.